Vibrational spectroscopy of $(SO_4^{2-})\cdot(H_2O)_n$ clusters, $n=1-5$: Harmonic and anharmonic calculations and experiment

Yifat Miller
Department of Physical Chemistry, The Hebrew University, Jerusalem 91904, Israel and Fritz Haber Research Center, The Hebrew University, Jerusalem 91904, Israel

Galina M. Chaban
NASA Ames Research Center, Moffett Field, California 94035

Jia Zhou
Department of Chemistry, University of California, Berkeley, California 94720 and Chemical Sciences Division, Lawrence Berkeley National Laboratory, Berkeley, California 94720

Knut R. Asmis
Institut für Experimentalphysik, Freie Universität Berlin, Arnimallee 14, D-14195 Berlin, Germany and Fritz-Haber-Institut der Max-Planck-Gesellschaft, Faradayweg 4-6, D-14195 Berlin, Germany

Daniel M. Neumark
Department of Chemistry, University of California, Berkeley, California 94720 and Chemical Sciences Division, Lawrence Berkeley National Laboratory, Berkeley, California 94720

R. Benny Gerber[a)]
Department of Physical Chemistry, The Hebrew University, Jerusalem 91904, Israel; Fritz Haber Research Center, The Hebrew University, Jerusalem 91904, Israel; and Department of Chemistry, University of California, Irvine, California 92697

(Received 21 May 2007; accepted 29 June 2007; published online 4 September 2007)

The vibrational spectroscopy of $(SO_4^{2-})\cdot(H_2O)_n$ is studied by theoretical calculations for $n=1-5$, and the results are compared with experiments for $n=3-5$. The calculations use both *ab initio* MP2 and DFT/B3LYP potential energy surfaces. Both harmonic and anharmonic calculations are reported, the latter with the CC-VSCF method. The main findings are the following: (1) With one exception (H_2O bending mode), the anharmonicity of the observed transitions, all in the experimental window of 540–1850 cm^{-1}, is negligible. The computed anharmonic coupling suggests that intramolecular vibrational redistribution does not play any role for the observed linewidths. (2) Comparison with experiment at the harmonic level of computed fundamental frequencies indicates that MP2 is significantly more accurate than DFT/B3LYP for these systems. (3) Strong anharmonic effects are, however, calculated for numerous transitions of these systems, which are outside the present observation window. These include fundamentals as well as combination modes. (4) Combination modes for the $n=1$ and $n=2$ clusters are computed. Several relatively strong combination transitions are predicted. These show strong anharmonic effects. (5) An interesting effect of the zero point energy (ZPE) on structure is found for $(SO_4^{2-})\cdot(H_2O)_5$: The global minimum of the potential energy corresponds to a C_s structure, but with incorporation of ZPE the lowest energy structure is C_{2v}, in accordance with experiment. (6) No stable structures were found for $(OH^-)\cdot(HSO_4^-)\cdot(H_2O)_n$, for $n\leqslant 5$. © *2007 American Institute of Physics*. [DOI: 10.1063/1.2764074]

I. INTRODUCTION

One of the motivations for interest in hydrates of the sulfate dianion (SO_4^{2-}) is the presence of the species in the atmosphere, as in aerosol particles.[1,2] Sulfate aerosols can act as cloud condensation nuclei leading to the formation of water droplets.[3] A detailed study of hydrated sulfate dianion clusters $(SO_4^{2-})\cdot(H_2O)_n$ can be very useful in this context by providing insights into the stepwise hydration of multiply charged anions. Thus, determination of the structures, vibrational properties, and interactions of these clusters is desirable.

Hydrated sulfate dianion clusters were first observed in the gas phase by Blades and Kebarle.[4] Several mass-spectrometric studies were reported.[5–9] An important step forward was the recent success in measuring vibrational spectroscopy in the infrared (IR) region of such clusters.[10,11] The frequencies and intensities of size-selected $(SO_4^{2-})\cdot(H_2O)_n$ clusters are expected to be sensitive to the potential energy surfaces. This calls for attempts at quantitative theoretical calculations that can test interaction potentials by comparison with experiment and can analyze their

[a)]Author to whom correspondence should be addressed. Fax: 972-2-6513742. Electronic mail: benny@fh.huji.ac.il

properties. Interaction potentials supported by spectroscopic experiments are valuable also for condensed-phase studies of the sulfate dianion in water solution. Molecular dynamics simulations of aqueous solutions of SO_4^{2-} using empirical force field have been reported recently.[12–14] The study of $(SO_4^{2-})\cdot(H_2O)_n$ with its rigorous spectroscopic basis should be also useful for future assessment of the force fields employed in such simulations.

The objective of the present paper is to explore the vibrational properties of $(SO_4^{2-})\cdot(H_2O)_n$ and, in particular, to compare the spectroscopic calculations with the IR spectroscopy experiments of Zhou *et al.*,[10] in order to learn about the potential energy surfaces governing the sulfate-water interaction. For example, both *ab initio* (MP2) and density functional theory (DFT) (B3LYP) potentials will be compared with experimental results. A number of electronic structure calculations of hydrated sulfate dianion clusters were reported in the literature.[7,13–17] In the present study, we will employ in some parts of the calculations the vibrational self-consistent field (VSCF) method[18–20] and specifically the correlation-corrected VSCF (CC-VSCF) algorithm. This method has the advantage that it computes the spectrum with the inclusion of anharmonic effects. Furthermore, the algorithm can be applied directly to potential surfaces from electronic structure codes,[18–20] which are not available analytically. It is of interest to explore the role of anharmonic effects on the vibrational spectroscopy in these systems. We note that VSCF and CC-VSCF have been successfully used for a range of similar or related systems. In particular, the method was recently employed by Chaban *et al.* to compute the IR and Raman spectra of hydrated magnesium sulfate salts.[21]

The structure of this paper is as follows. The methodology is presented in Sec. II. Section III describes the comparison of the spectroscopic calculations with experiment. Section III also presents the importance of anharmonic effects for the clusters studied here. Conclusions are presented in Sec. IV.

II. METHODS

Harmonic frequency calculations were carried out using the second-order perturbation level of theory[22] (MP2) using the TZP basis set: Dunning's basis set for O and H atoms[23] and the McLean-Chandler basis set for S atom.[24] The anharmonic vibrational spectroscopy calculations were carried out by the VSCF method and the CC-VSCF variant.[18–20] These methods have been described extensively in the literature.[25–42] The VSCF approximation includes anharmonic effects but makes the approximation that the vibrational wave functions are separable in the normal modes. The CC-VSCF method goes beyond separability of the wave functions and includes correlation effects between different normal modes. Thus, the CC-VSCF method treats both the intrinsic anharmonicity of each mode and the effects due to anharmonic coupling between different normal modes. The CC-VSCF approximation can be used directly with potential points generated from *ab initio* calculations as it applies here.[21] Both harmonic and anharmonic calculations using MP2 with the TZP basis set were performed using the GAMESS package of codes.[43] In addition, harmonic analysis was performed for the DFT, using the B3LYP functional with the TZVP+ basis set (similar basis set used for *ab initio* MP2 calculations), as implemented in the GAUSSIAN package of electronic structure programs.[44] The comparison of both MP2 and DFT results with experiment is important, as this can serve as a test of the relative accuracy of these two important electronic structure methods in the case of the ionic clusters studied here.

III. RESULTS AND ANALYSIS

A. Structures

The equilibrium structures of gas-phase hydrated sulfate dianion clusters, $(SO_4^{2-})\cdot(H_2O)_n$, $n=1-5$ were obtained by using the *ab initio* MP2/TZP level,[22–24] and can be seen in Fig. 1. The gas-phase $(SO_4^{2-})\cdot(H_2O)_2$ has two equilibrium structures that correspond to minima of the potential energy surface [Figs. 1(b) and 1(c)]. The global minimum structure of $(SO_4^{2-})\cdot(H_2O)_2$ is shown in Fig. 1(c) and the local minimum structure is shown in Fig. 1(b). The difference between the total energy of these two structures, not including the zero point energy, is 0.28 kcal/mol, while including the zero point energy, the total energy difference between these two structures is 0.33 kcal/mol. The structures described in Fig. 1 for $n=3$ and $n=4$ are the lowest energy isomers, as reported previously.[7] For $n=5$, two equilibrium structures had been computed [Figs. 1(f) and 1(g)]. The global minimum structure for $n=5$ is shown in Fig. 1(g) and differs from the lowest energy isomer reported previously by Wang *et al.*[7] The difference between the total energy including the zero point energy of these two structures is 0.5 kcal/mol. This topic is discussed in detail in Sec. III C. Earlier, Miller *et al.*[45] calculated the equilibrium structures of H_2SO_4 and its hydrate using the *ab initio* MP2/TZP level of theory. The computed geometric parameters obtained in that study[45] are in accordance with experimental values. Thus, we use here the same level of theory to compute the optimized geometries of $(SO_4^{2-})\cdot(H_2O)_n$, $n=1-5$. Geometry optimization were also performed using the DFT/B3LYP level for $(SO_4^{2-})\cdot(H_2O)_n$, $n=3-5$. The computed structures of the clusters studied here, using DFT/B3LYP-TZVP+ method, are similar to those obtained by *ab initio* MP2/TZP level of theory.

B. Comparison of harmonic MP2/TZP level of theory and harmonic DFT/B3LYP with experiment

Tables I–III compare the harmonic fundamental transitions obtained at the MP2/TZP and DFT/B3LYP level of theory to experimental data for $(SO_4^{2-})\cdot(H_2O)_3$, $(SO_4^{2-})\cdot(H_2O)_4$, and $(SO_4^{2-})\cdot(H_2O)_5$, respectively. For all clusters, the deviations from experiment of harmonic MP2 method are smaller than those at the harmonic DFT level of theory. Using the harmonic MP2 method, the deviations from experiment for $(SO_4^{2-})\cdot(H_2O)_3$, $(SO_4^{2-})\cdot(H_2O)_4$, and $(SO_4^{2-})\cdot(H_2O)_5$ are 2%, 2%, and 1%, respectively. On the other hand, deviations from experiment using the harmonic

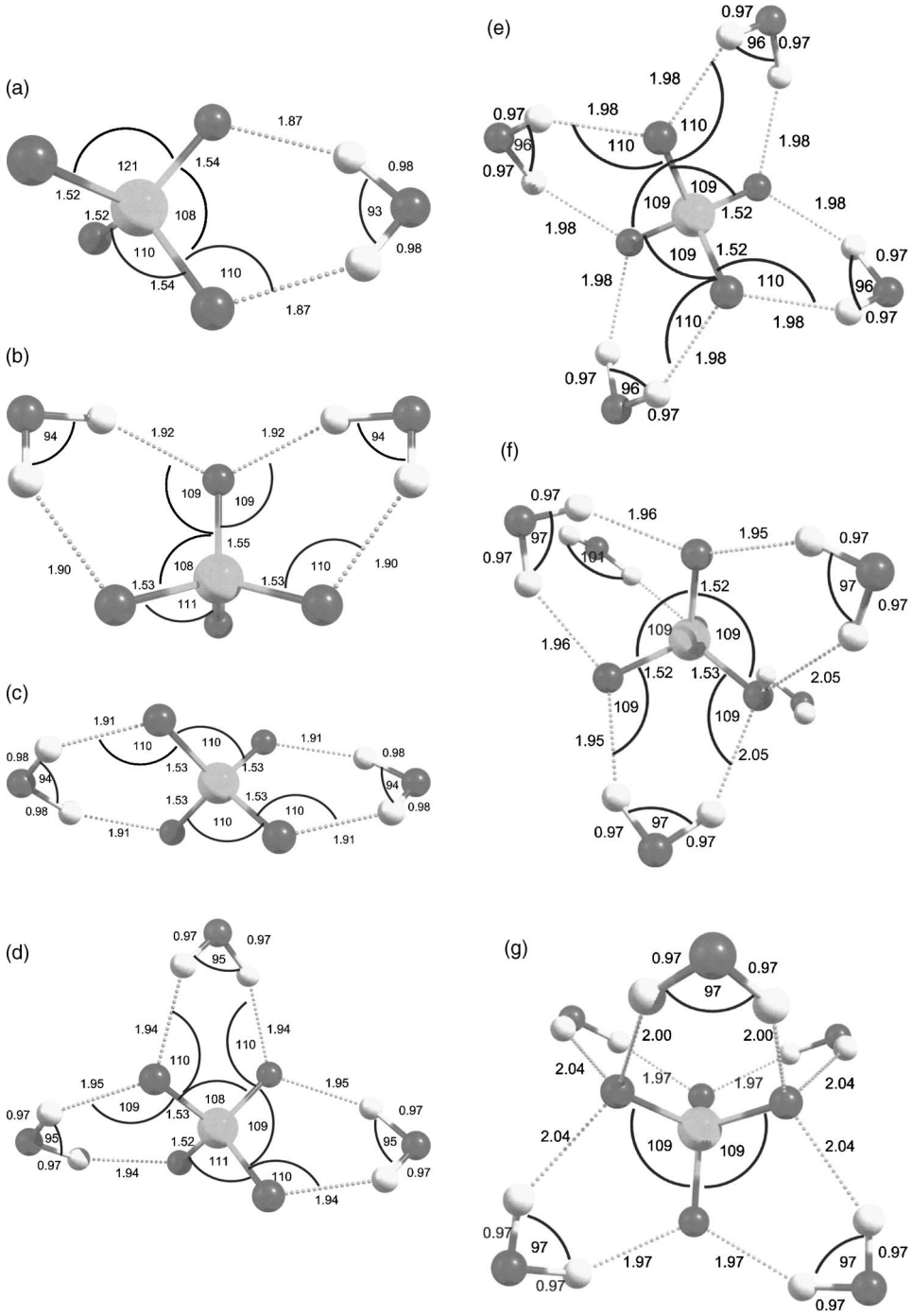

FIG. 1. The optimized equilibrium structure of (a) $(SO_4^{2-})\cdot(H_2O)$, (b) conformer 1 (local minimum) of $(SO_4^{2-})\cdot(H_2O)_2$, (c) conformer 2 (global minimum) of $(SO_4^{2-})\cdot(H_2O)_2$, (d) $(SO_4^{2-})\cdot(H_2O)_3$, (e) $(SO_4^{2-})\cdot(H_2O)_4$, (f) local C_s isomer of $(SO_4^{2-})\cdot(H_2O)_5$, and (g) global C_{2v} isomer of $(SO_4^{2-})\cdot(H_2O)_5$. Bond lengths (in angstroms) and angles (in degrees) are given for the *ab initio* MP2/TZP level.

DFT/B3LYP method for $(SO_4^{2-})\cdot(H_2O)_3$, $(SO_4^{2-})\cdot(H_2O)_4$, and $(SO_4^{2-})\cdot(H_2O)_5$ are 3%, 4%, and 2%, respectively. The mean deviation of the MP2 spectroscopic calculations from experiment is substantially smaller than that for DFT. We conclude that the MP2 potential surfaces are significantly more accurate than the DFT ones for these systems. While the structures obtained by these two methods are very similar, the vibrational frequencies obtained from the MP2 are in better agreement with experiment than those obtained from DFT, and the differences are systematic.

C. Zero point energy effects and the structure of $(SO_4^{2-})\cdot(H_2O)_5$

The lowest energy structures are important for understanding the solvation of SO_4^{2-}. Two structures of $(SO_4^{2-})\cdot(H_2O)_5$ corresponding to minima of the potential energy surface are found in the MP2 calculations. The first is the C_s isomer, shown in Fig. 1(f), and the second structure, shown in Fig. 1(g), is the C_{2v} isomer. The lowest energy optimized structure reported by Wang *et al.*[7] is similar to the C_s structure computed in the present study. Indeed, the C_s

TABLE I. Comparison between harmonic MP2, harmonic DFT, and experimental frequencies for $(SO_4^{2-})\cdot(H_2O)_3$.

Assignment	Harmonic MP2/TZP (cm^{-1})	Harmonic DFT/B3LYP (cm^{-1})	Experiment (cm^{-1})
Bend of water	1746	1722	1735
SO_2 asymmetric stretching	1094	1040	1102
SO_2 symmetric stretching	1058	1008	1052
SO_2 asymmetric stretching	1016	971	1080
$S-O_4$ stretching	913	866	943
Libration of water	869	837	862
SO_2 bending	589	569	613

structure is the global minimum of the MP2 potential energy surface and is more stable than the C_{2v} isomer by ~0.1 kcal/mol. However, the symmetric C_{2v} solvated cluster, in which each water molecule acts as double donor to the two sulfate O atoms, turns out to be the lowest energy structure when zero point energy (ZPE) is included. With incorporation of ZPE, the C_{2v} isomer is more stable than the C_s isomer by ~0.5 kcal/mol. Addition of the ZPE to the MP2 potential energy surface thus affects the findings of the global minimum and increases the energy difference between the C_{2v} and C_s isomers. The relative stability of the C_{2v} and the C_s structures for $(SO_4^{2-})\cdot(D_2O)_5$ is also affected by ZPE. When the ZPE calculation is included, the results show that the C_{2v} isomer is also the global minimum in the deuterated case. The C_{2v} isomer is more stable than the C_s isomer by ~0.3 kcal/mol for the deuterated case. Obviously, the ZPE effect for the deuterated complex is smaller, and therefore the relative stability of C_{2v} isomer compared with C_s is less pronounced than for the hydrogen isotopes, but in both cases C_{2v} is a more stable structure.

The result, including the ZPE effect, is in accordance with the experiment by Zhou *et al.*[10] Figure 2 compares the computed spectra of the C_{2v} and the C_s isomer to the measured spectra of $(SO_4^{2-})\cdot(H_2O)_5$. The harmonic frequencies of the C_{2v} and the C_s isomer are shown in Tables IV and V, respectively. One can see that the peak positions in both computed spectra are similar, except the peak at 845 cm^{-1}, which appears in the spectrum of C_s isomer but does not appear in the spectrum of C_{2v} isomer. This peak is assigned to a librational mode of H_2O. The temperature used in the experiment is very low (17 K). Although the energy difference between the two isomers is less than 1 kcal/mol, the low temperature used in the experiment does not allow seeing both C_{2v} and C_s isomers in the measured spectrum. However, it should be noted here that at higher temperatures, these two isomers may be seen in the spectrum for $(SO_4^{2-})\cdot(H_2O)_5$.

TABLE II. Comparison between harmonic MP2, harmonic DFT, and experiment frequencies for $(SO_4^{2-})\cdot(H_2O)_4$.

Assignment	Harmonic MP2/TZP (cm^{-1})	Harmonic DFT/B3LYP (cm^{-1})	Experiment (cm^{-1})
Bend of water	1768	1747	1714
SO_2 asymmetric stretching	1061	1013	1078
Libration of water	814	798	819

TABLE III. Comparison between harmonic MP2, harmonic DFT, and experiment frequencies for $(SO_4^{2-})\cdot(H_2O)_5$ [global minimum—Fig. 1(g): C_{2v} isomer].

Assignment	Harmonic MP2/TZP (cm^{-1})	Harmonic DFT/B3LYP (cm^{-1})	Experiment (cm^{-1})
Bend of water	1732	1719	1705
SO_2 asymmetric stretching	1090	1029	1081
Libration of water	782	778	792

D. *Ab initio* CC-VSCF calculations: Importance of the anharmonic effects

The fundamental harmonic and anharmonic transitions for $(SO_4^{2-})\cdot H_2O$ and for the two structures of $(SO_4^{2-})\cdot(H_2O)_2$ are shown in Tables VI–VIII. The intensities described in these tables are obtained from the anharmonic CC-VSCF approximation. However, experimental data for these clusters are not available. Wang *et al.*[7] suggested that in the gas phase, it requires at least three water molecules to stabilize significantly the sulfate dianion (SO_4^{2-}). The computed fundamental frequencies compared to experimental transitions for $(SO_4^{2-})\cdot(H_2O)_3$, $(SO_4^{2-})\cdot(H_2O)_4$, and $(SO_4^{2-})\cdot(H_2O)_5$ are shown in Tables IX, X, and IV, respectively. In the smaller cluster $(SO_4^{2-})\cdot(H_2O)_3$, both the frequencies and the intensities listed in Table IX are obtained from the CC-VSCF anharmonic method, while those of the larger clusters shown in Tables IV and X are computed using the harmonic approximation.

It is seen from Table IX that within the frequency range probed by Zhou *et al.*,[10] which did not include the OH stretches, the deviations from experiment are small for both

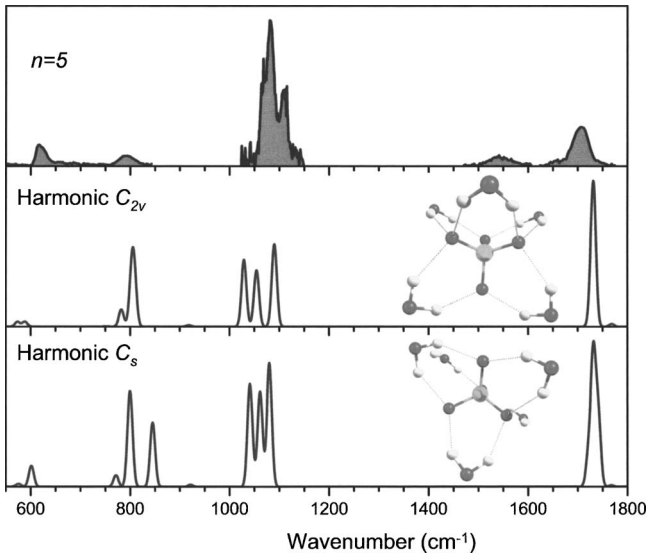

FIG. 2. The computed harmonic spectra for C_{2v} and C_s isomers of $(SO_4^{2-})\cdot(H_2O)_5$ vs the experimental measured spectrum (Ref. 9).

TABLE IV. Comparison between computed MP2-TZP harmonic and experiment frequencies for $(SO_4^{2-})\cdot(H_2O)_5$ [global minimum—Fig. 1(g): C_{2v} isomer].

Assignment	Harmonic frequencies (cm^{-1})	Experiment (cm^{-1})	Harmonic intensities (km/mol)
OH stretching	3790		96
OH stretching	3788		0
OH stretching	3782		290
OH stretching	3779		0
OH stretching	3770		120
OH stretching	3754		315
OH stretching	3746		40
OH stretching	3740		300
OH stretching	3737		768
OH stretching	3736		0
Bend of water	1768		23
Bend of water	1732	1705	561
Bend of water	1732		466
Bend of water	1727		238
Bend of water	1721		0
SO_2 asymmetric stretching	1090	1081	667
SO_2 symmetric stretching	1054		456
SO_2 asymmetric stretching	1029		540
$S-O_4$ stretching	918		12
Libration of water	808		336
Libration of water	803		392
Libration of water	782	792	138
Libration of water	752		3
Libration of water	747		0
Libration of water	588		41
SO_2 bending	574		25
SO_2 bending	572		16
SO_2 bending	451		0
Intermolecular	402		199
Intermolecular	402		151

TABLE V. Comparison between computed MP2-TZP harmonic and experimental frequencies for $(SO_4^{2-})\cdot(H_2O)_5$ [Local minimum—Fig. 1(f): C_s isomer].

Assignment	Harmonic frequencies (cm^{-1})	Experiment (cm^{-1})	Harmonic intensities (km/mol)
OH stretching	3834		167
OH stretching	3787		29
OH stretching	3779		195
OH stretching	3768		119
OH stretching	3747		323
OH stretching	3725		295
OH stretching	3720		113
OH stretching	3596		131
OH stretching	3680		503
OH stretching	3628		457
Bend of water	1767		8
Bend of water	1741	1705	362
Bend of water	1732		404
Bend of water	1730		283
Bend of water	1721		167
SO_2 asymmetric stretching	1080	1081	638
SO_2 symmetric stretching	1041		531
SO_2 asymmetric stretching	1061		491
$S-O_4$ stretching	921		11
Libration of water	845		331
Libration of water	800		359
Libration of water	798	792	145
Libration of water	771		60
Libration of water	757		0
Libration of water	611		0
SO_2 bending	601		108
SO_2 bending	577		11
SO_2 bending	572		6
Intermolecular	490		141
Intermolecular	417		218

harmonic and anharmonic methods. The anharmonic corrections provide an improvement over the harmonic model only for the bending mode of the water. Similarly, for the larger clusters, as may be seen in Tables IV and X, the deviations of the harmonic frequencies from experimental data are 2% and 1% for $n=4$ and $n=5$, respectively. The results are encouraging for the use of *ab initio* MP2/TZP level of theory for these clusters (not only in the context of anharmonic calculations). In fact, for these transitions the anharmonic corrections are only a small fraction of the error due to the potential function.

Figure 3 compares the computed spectrum of $(SO_4^{2-})\cdot(H_2O)_3$, including all the anharmonic fundamental frequencies and intensities to the measured spectrum and the computed harmonic spectrum of $(SO_4^{2-})\cdot(H_2O)_4$ to the measured spectrum, in the range from 540–1850 cm^{-1} obtained by Zhou *et al.*[10] The strong transitions in these measured spectra are for the following vibrations: bend of water ($\sim$1700 cm^{-1}), SO_2 asymmetric stretching mode ($\sim$1100 cm^{-1}), and libration of the water molecules ($\sim$700 cm^{-1}). The measured spectra are limited to the range of 540–1850 cm^{-1}. As seen from Fig. 3, for $n=3$, the computed spectrum is qualitatively similar to the measured spectrum. The measured peak at 1735 cm^{-1} is similar to the strong transition in the computed spectrum (1711 cm^{-1}). The three peaks in the measured spectrum 1102, 1079, and 1052 cm^{-1} have relatively similar intensities as the computed transitions: 1076, 1043, and 1000 cm^{-1}. Finally, the transition in the measured spectrum at 613 cm^{-1} appears also in the computed spectrum at 585 cm^{-1}. More quantitative comparison of intensities requires treatment of the rotational effects in the spectrum. Such calculations were not attempted here. Quantitative comparison with experiment, e.g., in the context of testing the accuracy of the potential, is therefore based on the frequencies of the assigned transition.

It is of interest to comment here also on strong transi-

TABLE VI. Comparison between MP2-TZP harmonic and anharmonic frequencies for $(SO_4^{2-})\cdot(H_2O)$.

Assignment	Harmonic (cm^{-1})	VSCF (cm^{-1})	CC-VSCF (cm^{-1})	Anharmonic intensities (km/mol)
OH symmetric stretching	3592	3354	3286	579
OH asymmetric stretching	3541	3137	3039	163
Bend of water	1765	1717	1701	383
SO_2 asymmetric stretching	1095	1081	1078	551
SO_2 symmetric stretching	1060	1051	1045	613
SO_2 asymmetric stretching	1003	989	986	391
Libration of water	932	962	930	183
$S-O_4$ stretching	904	897	892	17
SO_2 bending	585	580	580	85
SO_2 bending	580	575	575	54
SO_2 bending	569	566	566	44
Intermolecular	532	569	601	100
Intermolecular	505	578	587	0
Intermolecular	430	427	427	4
Intermolecular	397	399	395	0
Intermolecular	231	229	229	22
Intermolecular	128	138	113	5
Intermolecular	43	56	55	0

tions in other ranges of the computed spectra. As may be seen in Table IX and Fig. 3, indeed, the three transitions of the above mentioned vibrations in $(SO_4^{2-})\cdot(H_2O)_3$ are strong. However, strong transitions may be predicted also for the OH symmetric stretching vibration and for the OH asymmetric stretching vibration (Table IX). These strong transitions appear both in the smaller clusters (Tables VI–VIII) and in the larger clusters (Tables IV, IX, and X).

For all the clusters studied here strong intermolecular transitions also appear in the predicted spectra (Tables IV–X). At least one intermolecular transition in each spectrum seems to be a strong transition and, in principle, should be experimentally measurable. Thus, the peak at 430 cm^{-1} in the spectrum of $(SO_4^{2-})\cdot(H_2O)_4$ is one of the intermolecular modes and has intensity of 225 km/mol (Table X). Another

TABLE VII. Comparison between MP2-TZP harmonic and anharmonic frequencies for $(SO_4^{2-})\cdot(H_2O)_2$ [local minimum-Fig. 1(b)].

Assignment	Harmonic (cm^{-1})	VSCF (cm^{-1})	CC-VSCF (cm^{-1})	Anharmonic intensities (km/mol)
OH symmetric stretching	3654	3449	3367	283
OH symmetric stretching	3644	3410	3382	614
OH asymmetric stretching	3625	3384	3348	337
OH asymmetric stretching	3617	3363	3332	23
Bend of water	1771	1732	1722	267
Bend of water	1747	1707	1706	427
S–O stretch	1114	1100	1098	591
SO_2 asymmetric stretching	1056	1040	1037	582
SO_2 symmetric stretching	997	987	981	365
Libration of water with $S-O_4$ str.	907	932	925	175
SO_2 sym. str. with libration of water	898	946	932	198
Libration of water	878	948	929	62
SO_2 bending	585	581	580	66
SO_2 bending	583	579	578	80
SO_2 bending	567	565	565	35
Intermolecular	505	614	568	95
Intermolecular	499	585	544	51
Intermolecular	485	603	556	72

TABLE VIII. Comparison between MP2-TZP harmonic and anharmonic frequencies for $(SO_4^{2-})\cdot(H_2O)_2$ [global minimum-Figure 1(c)].

Assignment	Harmonic (cm^{-1})	VSCF (cm^{-1})	CC-VSCF (cm^{-1})	Anharmonic intensities (km/mol)
OH symmetric stretching	3648	3459	3360	0
OH symmetric stretching	3641	3415	3291	985
OH asymmetric stretching	3617	3224	3118	145
OH asymmetric stretching	3617	3224	3118	145
Bend of water	1764	1726	1712	0
Bend of water	1753	1715	1705	715
SO_2 symmetric stretching	1064	1054	1051	745
SO_2 asymmetric stretching	1049	1035	1032	440
SO_2 asymmetric stretching	1049	1035	1032	440
$S-O_4$ stretching	912	906	900	0
Libration of water	891	946	924	192
Libration of water	891	946	924	192
SO_2 bending	591	586	586	112
SO_2 bending	573	569	569	39
SO_2 bending	573	569	569	39
Intermolecular	497	579	533	104
Intermolecular	497	579	533	104

pronounced intermolecular mode is the peak at 402 cm^{-1} in the spectrum of $(SO_4^{2-})\cdot(H_2O)_5$, which has intensity of 199 km/mol (Table IV).

From CC-VSCF calculations, it is possible to compute the contribution for each transition of the intrinsic anharmonicity of a given mode and the contribution of anharmonic coupling. The algorithm to compute the contribution of the intrinsic single-mode anharmonicity to the frequency and the

TABLE IX. Comparison between MP2-TZP harmonic, anharmonic and experimental frequencies for $(SO_4^{2-})\cdot(H_2O)_3$.

Assignment	Harmonic (cm^{-1})	VSCF (cm^{-1})	CC-VSCF (cm^{-1})	Experiment (cm^{-1})	Anharmonic intensities (km/mol)
OH symmetric stretching	3698	3511	3414		59
OH asymmetric stretching	3691	3435	3396		237
OH symmetric stretching	3687	3468	3454		430
OH symmetric stretching	3683	3481	3463		776
OH asymmetric stretching	3679	3437	3380		70
OH asymmetric stretching	3675	3439	3410		83
Bend of water	1770	1737	1727		80
Bend of water	1746	1713	1711	1735	646
Bend of water	1738	1704	1699		252
SO_2 asymmetric stretching	1094	1079	1076	1102	629
SO_2 symmetric stretching	1058	1049	1043	1079	522
SO_2 asymmetric stretching	1016	1003	1000	1052	444
$S-O_4$ stretching	913	907	901	943	19
Libration of water	869	951	936	862	391
Libration of water	852	930	913		189
Libration of water	833	922	905		31
SO_2 bending	589	585	585	613	95
SO_2 bending	580	576	576		59
SO_2 bending	567	565	565		27
Intermolecular	470	590	550		100
Intermolecular	464	591	555		76
Intermolecular	460	543	490		89

TABLE X. Comparison between MP2–TZP computed harmonic and experimental frequencies for $(SO_4^{2-})\cdot(H_2O)_4$.

Assignment	Harmonic frequencies (cm^{-1})	Experiment (cm^{-1})	Harmonic intensities (km/mol)
OH stretching	3739		159
OH stretching	3734		0
OH stretching	3733		15
OH stretching	3733		15
OH stretching	3726		0
OH stretching	3722		801
OH stretching	3722		801
OH stretching	3720		0
Bend of water	1768	1714	0
Bend of water	1739		559
Bend of water	1739		559
Bend of water	1727		0
SO_2 asymmetric stretching	1061	1078	660
SO_2 symmetric stretching	1046		374
SO_2 asymmetric stretching	1061		660
$S-O_4$ stretching	918		0
Libration of water	843		334
Libration of water	814	819	168
Libration of water	814		168
Libration of water	782		0
SO_2 bending	586		46
SO_2 bending	586		46
SO_2 bending	565		9
Intermolecular	430		225
Intermolecular	428		104
Intermolecular	428		104

contribution of the anharmonic coupling element between modes is detailed by Miller *et al.*[45] The computation of these contributions was carried out here for $(SO_4^{2-})\cdot(H_2O)_n$, $n=1-3$. In all these clusters, the coupling contributions to the fundamental of the OH symmetric stretching vibration and the OH asymmetric stretching vibration are greater than the intrinsic single-mode anharmonicities. For the smaller cluster $(SO_4^{2-})\cdot(H_2O)$, the value of the anharmonic coupling contribution for the OH symmetric stretching vibration is 209 cm^{-1}, while for the OH asymmetric stretching vibration it is 602 cm^{-1}. The large contributions of the anharmonic coupling between modes for both OH asymmetric and symmetric stretching vibrations also appear for the larger clusters. The anharmonic contribution of coupling for the local minimum of $(SO_4^{2-})\cdot(H_2O)_2$ is 235–239 cm^{-1}, while for the global minimum of $(SO_4^{2-})\cdot(H_2O)_2$, its values are in the range between 241 and 595 cm^{-1}. For $(SO_4^{2-})\cdot(H_2O)_3$, the values of anharmonic coupling corrections becomes smaller but still fairly large (248–350 cm^{-1}).

The anharmonic coupling between different modes is of considerable interest in intramolecular vibrational redistribution, since effects may appear between modes. Therefore, the magnitude of the coupling between modes and analysis of their behavior may be studied. Recently, Miller *et al.*[45] computed the average absolute values of the coupling potential for H_2SO_4 and $H_2SO_4\cdot H_2O$. The definition of the average absolute value of the coupling potential is given by

$$\overline{V_{ij}}(Q_i,Q_j)=\langle\Psi_i(Q_i)\Psi_j(Q_j)\|V_{ij}(Q_i,Q_j)\|\Psi_i(Q_i)\Psi_j(Q_j)\rangle. \quad (1)$$

Here, Q_i and Q_j are the normal-mode coordinates for modes i and j, and Ψ_i and Ψ_j are the ground state wave functions. In this study, we use this algorithm to compute the average absolute values of the coupling potential for $(SO_4^{2-})\cdot(H_2O)_n$ clusters. The magnitude of the coupling integral between the OH symmetric stretching vibration and a few normal modes in $(SO_4^{2-})\cdot(H_2O)_n$, $n=1-3$, are shown in Figs. 4–7, using the MP2/TZP potential. Only the couplings of the OH symmetric stretching vibrational mode with modes which are strong and important appear in these figures. As seen from Figs. 4–7, the largest magnitude of the coupling integral for all the clusters $(SO_4^{2-})\cdot(H_2O)_n$, $n=1-3$, is between the OH symmetric stretching vibration and the OH asymmetric stretching vibration. The OH symmetric stretching vibration also strongly couples to a few of intermolecular modes for the small clusters $(SO_4^{2-})\cdot(H_2O)$ and $(SO_4^{2-})\cdot(H_2O)_2$ (Figs. 4–6). Neither the OH stretching vibra-

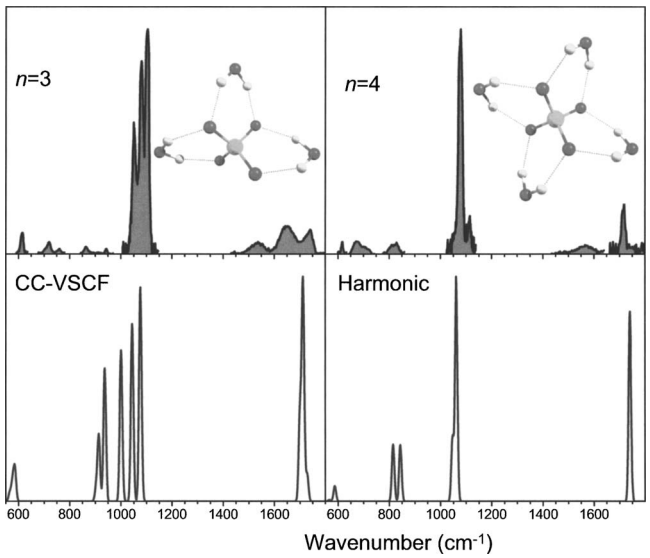

FIG. 3. The computed anharmonic spectrum for $(SO_4^{2-})\cdot(H_2O)_3$ and harmonic spectrum for $(SO_4^{2-})\cdot(H_2O)_4$ vs the experimental measured spectra for each cluster (Ref. 9).

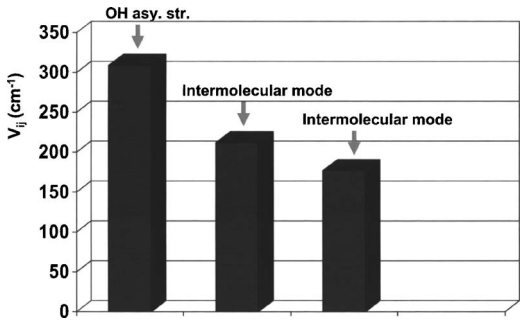

FIG. 4. Magnitude of the coupling integral between the OH symmetric stretching vibration with other modes in $(SO_4^{2-})\cdot H_2O$.

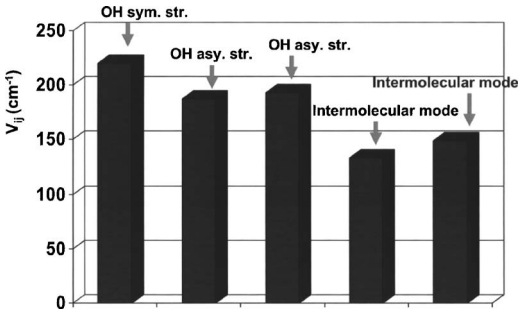

FIG. 5. Magnitude of the coupling integral between the OH symmetric stretching vibration with other modes in the conformer 1 of $(SO_4^{2-})\cdot(H_2O)_2$.

tions nor the intermolecular modes are in the range of the measured spectra. Thus, we predict here that anharmonicity effects are important in the range larger than 1850 cm^{-1} and smaller than 540 cm^{-1}. These results may have important implications for internal vibrational energy flow and intramolecular dynamics.

E. Combination transitions

Computing overtone and combination transitions for systems of more than several atoms, such as $(SO_4^{2-})\cdot(H_2O)_n$, $n=1-3$, is fairly challenging. The interesting question is whether the combination transitions in these systems are strong enough to be measured by experiment. The CC-VSCF method has been proven[42,45] to work well for low overtones and combination transitions. It has been observed that the results obtained by the anharmonic CC-VSCF approximation are in accordance with experiment and that the improvement of this method over the harmonic approximation is fairly large.

Strong values of intensities of combination modes indicate strong coupling between modes. In fact, in the cases where the couplings are strong, the dipole moment and the transition moments are large. Tables IX and XI describe the largest theoretical intensities obtained by the CC-VSCF calculations for $(SO_4^{2-})\cdot(H_2O)$ and the global minimum $(SO_4^{2-})\cdot(H_2O)_2$, respectively. The most intense combination transitions include fundamental transition of OH stretching vibration and intermolecular mode (Tables XI and XII). However, combination modes which include first overtone of OH stretching vibration and fundamental transition of bending of water or SO_2 asymmetric stretching vibration or SO_2 symmetric stretching vibration are even more important and have intensities between 21 and 66 km/mol.

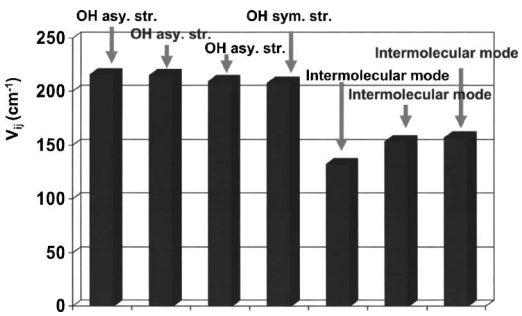

FIG. 6. Magnitude of the coupling integral between the OH symmetric stretching vibration with other modes in the conformer 2 of $(SO_4^{2-})\cdot(H_2O)_2$.

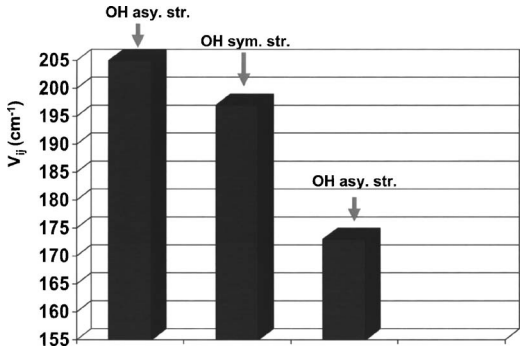

FIG. 7. Magnitude of the coupling integral between the OH symmetric stretching vibration with other modes in $(SO_4^{2-})\cdot(H_2O)_3$.

It should be noted here that the observed peak position in the IR spectra in the range of 1500–1600 cm^{-1} cannot be explained by our combination transition calculations and thus this assignment remains open.

F. Minimum structures for $(OH^-)\cdot(HSO_4^-)\cdot(H_2O)_n$

Local minima of the $(OH^-)\cdot(HSO_4^-)\cdot(H_2O)_n$ clusters $(n=1-3)$ have not been obtained using MP2/TZP calculations. During the optimization process, the H atom in HSO_4^- transfers to the OH^- to form H_2O. It seems that the $(SO_4^-)\cdot(H_2O)_n$ clusters are considerably more stable than $(OH^-)\cdot(HSO_4^-)\cdot(H_2O)_n$ clusters. Gao and Liu[16] computed the minimum structures of the $(HSO_4^-)\cdot(H_2O)_n+(OH)\cdot(H_2O)_n$, but so far, to the best of our knowledge, calculations of $(OH^-)\cdot(HSO_4^-)\cdot(H_2O)_n$ clusters had not been carried out. It seems that if the latter clusters exist, they do so only for larger n.

IV. SUMMARY AND CONCLUDING REMARKS

This paper studies the properties of hydrated sulfate ions on the basis of comparison between IR experiments and theoretical calculations at both harmonic and anharmonic levels. The spectroscopic results are found to be a sensitive probe of the structures of the anion hydrates and of the accuracy of the potential energy surfaces used.

TABLE XI. Anharmonic combination transitions for $(SO_4^{2-})\cdot(H_2O)$ using MP2-TZP level.

Mode 1	Mode 2	CC-VSCF (cm^{-1})	Anharmonic intensities (km/mol)
OH asymmetric stretching	Intermolecular mode	3229	20
First overtone of OH asy. str.	Bend of water	7759	29
First overtone of OH asy. str.	SO_2 asymmetric stretching	7339	21
First overtone of OH asy. str.	SO_2 symmetric stretching	7302	28

TABLE XII. Anharmonic combination transitions for the global minimum $(SO_4^{2-})\cdot(H_2O)_2$ using MP2-TZP level.

Mode 1	Mode 2	CC-VSCF (cm^{-1})	Anharmonic intensities (km/mol)
First overtone of OH asymmetric stretching	Bend of water	7611	53
First overtone of OH asymmetric stretching	SO_2 asymmetric stretching	7062	41
First overtone of OH asymmetric stretching	SO_2 symmetric stretching	7094	66

The results demonstrate that the MP2 and B3LYP potential energy surfaces are in very good accordance with the experimental frequencies. Also, the main intensity features are reproduced by the calculations, though the agreement on this is less quantitative than for the frequencies. The good agreement between experiment and theory strongly indicates that both MP2 and B3LYP provide a good description of the potential energy surfaces of the ion clusters studied here. The results may be of interest for the calibration of force fields for studies of sulfate ions in solution.

Both B3LYP and MP2 yield good agreement with experiment; however, the comparison shows that MP2 results are more accurate. The difference between the MP2 and B3LYP results is not large, but seems systematic for the three clusters studied here. It should be useful to examine this point also for other ion hydrates. Accurate description of potential energy surfaces of these systems is obviously important. High-resolution IR data, as were available here, are essential for this purpose, since comparison of calculations with experiments provides a rigorous test of the potential surfaces employed.

Part of the calculations carried out in this study focused on anharmonic effects, in order to study the possible role for coupling effects between different vibrational modes. With the exception of one or two transitions, the role of anharmonic effects in the experimental window used here was found to be negligible. On the other hand, substantial anharmonic effects were observed for transitions that are not accessible in the present experiment, as expected for hydrogen-bonded clusters. The results presented here may be of a use in interpreting the spectra which were investigated by Bush *et al.*[10] The prediction of several relatively strong combination mode transitions in these systems is of interest in this respect. Thus, combination transitions that will be explored experimentally to the systems studied here may throw light on the possible role of intramolecular vibrational dynamics in these systems.

ACKNOWLEDGMENTS

This research was supported by the U.S.-Israel Binational Science Foundation (BSF-2004009). It is also supported by NSF through the EMSI at UC Irvine (Grant No. 0431312), CRC project (0209719), and by a grant from the state of Lower Saxony and the Volkswagen Foundation, Hannover, Germany. One of the authors (D.M.N.) acknowledges support from the Air Force Office of Scientific Research under Grant No. F49620-03-1-0085. Two of the authors (K.R.A. and G.S.) gratefully acknowledge the support of the Stichting voor Fundamental Onderzoek der Materie (FOM) in providing the required beam time on FELIX and highly appreciate the skillful assistance of the FELIX staff. They also thank the Deutsche Forschungsgemeinschaft for support as part of the GK788 and the SFB546.

[1] B. J. Finlayson-Pitts and J. N. Pitts, Jr., *Chemistry of the Upper and Lower Atmosphere-Theory, Experiments, and Applications* (Academic, San Diego, 2000).
[2] S. Twomey, *Atmospheric Aerosols* (Elsevier, New York, 1977).
[3] R. Pincus and M. B. Baker, Nature (London) **372**, 250 (1994).
[4] A. T. Blades and P. Kebarle, J. Am. Chem. Soc. **116**, 10761 (1994).
[5] A. T. Blades, J. S. Klassen, and P. Kebarle, J. Am. Chem. Soc. **117**, 10563 (1995).
[6] A. T. Blades and P. Kebarle, J. Phys. Chem. A **109**, 8293 (2005).
[7] X. B. Wang, J. B. Nicholas, and L. S. Wang, J. Chem. Phys. **113**, 10837 (2000).
[8] X. B. Wang, X. Yang, J. B. Nicholas, and L. S. Wang, Science **294**, 1322 (2001).
[9] X. Yang, X. B. Wang, and L. S. Wang, J. Phys. Chem. A **106**, 7607 (2002).
[10] J. Zhou, G. Santambrogio, M. Brümmer, D. T. Moore, L. Wöste, G. Meijer, D. M. Neumark, and K. R. Asmis, J. Chem. Phys. **125**, 111102 (2006).
[11] M. F. Bush, R. J. Saykally, and E. R. Williams, J. Am. Chem. Soc. **129**, 2220 (2007).
[12] S. Gopalakrishnan, P. Jungwirth, D. J. Tobias, and H. C. Allen, J. Phys. Chem. B **109**, 8861 (2005).
[13] P. Jungwirth, J. E. Curtis, and D. J. Tobias, Chem. Phys. Lett. **367**, 704 (2003).
[14] R. L. Wong and E. R. Williams, J. Phys. Chem. A **107**, 10976 (2003).
[15] C. G. Zhan, F. Zheng, and D. A. Dixon, J. Chem. Phys. **119**, 781 (2003).
[16] B. Gao and Z. F. Liu, J. Chem. Phys. **121**, 8299 (2004).
[17] B. Gao and Z. F. Liu, J. Chem. Phys. **123**, 224302 (2005).
[18] J. O. Jung and R. B. Gerber, J. Chem. Phys. **105**, 10682 (1996).
[19] J. O. Jung and R. B. Gerber, J. Chem. Phys. **105**, 10332 (1996).
[20] G. M. Chaban, J. O. Jung, and R. B. Gerber, J. Chem. Phys. **111**, 1823 (1999).
[21] G. M. Chaban, W. M. Huo, and T. J. Lee, J. Chem. Phys. **117**, 2532 (2002).
[22] J. A. Pople, J. S. Binkley, and R. Seeger, Int. J. Quantum Chem. **10**, 1 (1976).
[23] T. H. Dunning, J. Chem. Phys. **55**, 716 (1971).
[24] A. D. McLean and G. C. Chandler, J. Chem. Phys. **72**, 5639 (1980).
[25] G. M. Chaban, J. O. Jung, and R. B. Gerber, J. Phys. Chem. A **104**, 2772 (2000).
[26] N. J. Wright, R. B. Gerber, and D. J. Tozer, Chem. Phys. Lett. **324**, 206 (2000).
[27] N. J. Wright and R. B. Gerber, J. Chem. Phys. **112**, 2598 (2000).
[28] S. K. Gregurick, G. M. Chaban, and R. B. Gerber, J. Phys. Chem. A **106**, 8696 (2002).
[29] R. B. Gerber, B. Brauer, S. K. Gregurick, and G. M. Chaban, PhysChemComm **5**, 142 (2002).
[30] G. M. Chaban and R. B. Gerber, J. Chem. Phys. **115**, 1340 (2001).
[31] G. M. Chaban, J. O. Jung, and R. B. Gerber, J. Phys. Chem. A **104**, 10035 (2000).
[32] G. M. Chaban, R. B. Gerber, and K. C. Janda, J. Phys. Chem. A **105**, 8323 (2001).
[33] G. M. Chaban and R. B. Gerber, Spectrochim. Acta, Part A **58**, 887 (2002).
[34] R. B. Gerber and J. O. Jung, in *Computational Molecular Spectroscopy*, edited by P. Jensen and P. R. Bunker (Wiley, Surrex, UK, 2000), pp. 365.
[35] S. Carter, S. J. Culik, and J. M. Bowman, J. Chem. Phys. **107**, 10458 (1997).
[36] B. Brauer, G. M. Chaban, and R. B. Gerber, Phys. Chem. Chem. Phys. **6**, 2543 (2004).

[37] R. B. Gerber, G. M. Chaban, S. K. Gregurick, and B. Brauer, Biopolymers **68**, 370 (2003).
[38] R. B. Gerber, G. M. Chaban, B. Brauer, and Y. Miller, in *Theory and Applications of Computational Chemistry: The First* 40 Years, edited by C. E. Dykstra, G. F., K. S. Kim, and G. E. Scuseria (Elsevier, Amsterdam, 2005), pp. 165.
[39] N. Matsunaga, G. M. Chaban, and R. B. Gerber, J. Chem. Phys. **117**, 3541 (2002).
[40] D. M. Benoit, J. Chem. Phys. **120**, 562 (2004).
[41] O. Christiansen, J. Chem. Phys. **120**, 2140 (2004).
[42] Y. Miller, G. M. Chaban, and R. B. Gerber, Chem. Phys. **313**, 213 (2005).
[43] http://www.msg.ameslab.gov/GAMESS/GAMESS.html
[44] M. J. Frisch, G. W. Trucks, H. B. Schlegel *et al.*, GAUSSIAN03, Gaussian, Inc., Wallingford CT, 2004.
[45] Y. Miller, G. M. Chaban, and R. B. Gerber, J. Phys. Chem. A **109**, 6565 (2005).